ESCUELA NAVAL DE CADETES
"ALMIRANTE PADILLA"
Honor y Tradición

OnBoard Knowledge Journal

Research article

Development of a Neural Network-Based Classifier for Child-hood Pneumonia Diagnosis Using Chest X-ray Images

Desarrollo de un clasificador basado en redes neuronales para el diagnóstico de neumonía infantil mediante imágenes de ra-yos X

Fredy Munera Romero[1]* Adrian Gómez Consuegra [1]

[1] Systems Engineering Program, Faculty of Engineering, Corporación Universitaria Rafael Núñez (Uninuñez) Cartagena, 130001, Colombia; fmunerar21@campusuninunez.edu.co; agomezc21@campusuninunez.edu.co

* Correspondence: fmunerar21@campusuninunez.edu.co

Citation: Munera, F., Gómez, A. Development of a Neural Network-Based Classifier for Child-hood Pneumonia Diagnosis Using Chest X-ray Images. *OnBoard Knowledge Journal* **2026**, 2, 8. https://doi.org/10.70554/OBJK2026.v02n01.08

Received: 18/03/2026, Accepted: 06/06/2026, Published: 16/06/2026

DOI: https://doi.org/10.70554/OBJK2026.v02n01.08

Abstract: This study presents the development of a neural network-based classifier for the diagnosis of childhood pneumonia using chest X-ray images. The database used contains anteroposterior radiographs from retrospective cohorts of pediatric patients aged one to five years from the Guangzhou Women and Children's Medical Center. Using a routine developed in MATLAB, seven texture features were extracted from each image: mean, standard deviation, entropy, contrast, correlation, energy, and homogeneity. These features were used as inputs for a feed-forward artificial neural network designed to classify the images as normal or associated with bacterial pneumonia. The database consisted of 49 normal images and 48 images with bacterial pneumonia. The best-performing neural network achieved an overall accuracy of 96.9%, suggesting that the proposed approach may constitute an efficient and interpretable tool to support computer-aided diagnosis. However, the reduced size of the dataset and the lack of external validation limit the clinical generalizability of the model, an aspect that should be addressed in future research.

Keywords: Classifier; Chest X-ray images; Pediatric pneumonia; Neural networks; Computer-aided diagnosis; Artificial intelligence

Resumen: Este estudio presenta el desarrollo de un clasificador basado en redes neuronales para el diagnóstico de neumonía infantil mediante imágenes de rayos X de tórax. La base de datos utilizada contiene radiografías anteroposteriores de cohortes retrospectivas de pacientes pediátricos de uno a cinco años del Centro Médico de Mujeres y Niños de Guangzhou. Mediante una rutina desarrollada en MATLAB, se extrajeron siete características de textura de cada imagen: media, desviación estándar, entropía, contraste, correlación, energía y homogeneidad. Estas características fueron utilizadas como entradas de una red neuronal artificial de alimentación directa, diseñada para clasificar las imágenes como normales o asociadas con neumonía bacteriana. La base de datos estuvo conformada por 49 imágenes normales y 48 imágenes con neumonía bacteriana. La red neuronal con mejor desempeño alcanzó una exactitud global

del 96.9%, lo que sugiere que el enfoque propuesto puede constituir una herramienta eficiente e interpretable de apoyo al diagnóstico asistido por computador. No obstante, el tamaño reducido del conjunto de datos y la ausencia de validación externa limitan la generalización clínica del modelo, aspecto que deberá abordarse en investigaciones futuras.

Palabras clave: Clasificador; Imágenes de rayos X de tórax; Neumonía infantil; Redes neuronales; Diagnóstico asistido por computador; Inteligencia artificial

1. Introduction

Pneumonia is an acute infection of the pulmonary parenchyma that can range from localized inflammation to fluid accumulation in the lungs. Its etiology may involve viral, bacterial, or fungal infections. It affects both non-hospitalized and hospitalized patients and is characterized by various clinical manifestations, including fever and respiratory symptoms (such as cough and expectoration), alongside observable alterations in chest X-ray images. Globally, this disease accounts for more than 15% of all deaths in children under five years of age [8].

In the United States, pneumonia led to over 500,000 emergency department visits and more than 50,000 deaths according to 2015 data, maintaining its position among the top ten leading causes of death worldwide [12].

Despite the existence of various prevention, diagnosis, and treatment measures, half of global childhood pneumonia deaths occur in Africa, particularly in Nigeria (210,000 deaths), the Democratic Republic of the Congo (132,000), and Ethiopia (114,000). In Asia, India accounts for 410,000 deaths, followed by Pakistan (92,000) and Afghanistan (89,000). Consequently, for every child who loses their life to pneumonia in a developed country, more than 2,000 die in a developing nation. According to the Clinical University Hospital of Santiago de Compostela (Spain) in the journal Neumo Expertos en Prevención, it is estimated that 150 million children develop the disease annually, with 11 million hospitalizations occurring almost exclusively in developing countries, such as Mexico [2]. As part of the global effort to combat such widespread health challenges, technology has made significant contributions. In this context, Artificial Intelligence (AI) plays a leading role by combining algorithms to create systems capable of providing human-like analytical capabilities and assistance [3].

Currently, Chest X-ray (CXR) imaging is widely recognized as a standard tool for pneumonia diagnosis. However, contemporary research focusing on data processing and predictive systems can further enhance diagnostic accuracy. Advanced technology pro-poses the implementation of Artificial Neural Networks (ANN), which are biologically inspired models composed of elements that function analogously to neurons and are organized in a manner similar to the human brain [1].

The primary objective of this article is to develop and evaluate a neural network-based classifier to support healthcare specialists in the diagnosis of pediatric pneumonia using chest X-ray images. The proposed model analyzes texture features extracted from radiological images to distinguish between normal cases and cases associated with bacterial pneumonia. In this way, the classifier is intended as a computer-aided decision-support tool, particularly relevant for healthcare environments where access to specialized radiological interpretation may be limited.

The article is structured as follows. Section 2 presents the main contributions of the study, emphasizing the development of an interpretable and computationally efficient computer-aided diagnosis approach for childhood pneumonia. Section 3 reviews previous studies on the use of artificial intelligence, machine learning, and deep learning techniques for pneumonia detection from chest X-ray images. Section 4 describes the dataset, the feature extraction process, the neural network classifier design, and the performance evaluation criteria used in the study. Section 5 presents the experimental findings, including the effect of hidden layer size on network performance, classification accuracy, confusion matrices, and training behavior. Section 6 analyzes the results in relation to previous research, highlighting the advantages, limitations, and future research directions of the proposed approach. Finally, Section 7 summarizes the main findings and

emphasizes the potential of simple feature-based neural network models as accessible and interpretable tools to support pediatric pneumonia diagnosis.

2. Contributions

This study presents a computer-aided diagnosis (CAD) system for childhood pneumonia that offers a balance between high performance and computational simplicity. The main contributions of this work to the existing body of knowledge are threefold:

ii. Unlike the current trend of applying complex and often opaque deep learning mod-els (such as convolutional neural networks) directly to raw images, this research demonstrates that a classical machine learning approach remains highly effective. By manually engineering a small set of seven texture features (mean, standard deviation, entropy, contrast, correlation, energy, and homogeneity) extracted via a MATLAB routine, we show that it is possible to achieve diagnostic accuracy exceeding 96.9% with a simple feed-forward neural network. This provides a more interpretable and less computationally expensive alternative for institutions with limited resources.

ii. The study provides a detailed empirical analysis of the neural network's architecture. By systematically varying the number of neurons in the hidden layer (from 3 to 9) and evaluating performance metrics like MSE, training time, and confusion matrices, we identify an optimal configuration (4 neurons) that maximizes accuracy while minimizing complexity and overfitting. This granular analysis offers practical insights for other researchers developing similar diagnostic tools.

ii. This work contributes a validated, low-cost tool to support clinical decision-making. The high precision (96.9%) achieved on a challenging dataset of pediatric chest X-rays positions this classifier as a reliable "second opinion" for specialists, potentially reducing diagnostic delays and improving patient outcomes, particularly in primary care settings where expert radiologists may not be immediately available.

3. Related Works

The application of artificial intelligence (AI) for pneumonia diagnosis using chest X-ray (CXR) images has been an active area of research, particularly in the pediatric population where the disease burden remains high. Recent advances in machine learning (ML) and deep learning (DL) have led to the development of numerous computer-aided diagnosis (CAD) systems aimed at improving diagnostic accuracy and reducing the workload of radiologists [13].

Several recent studies have demonstrated the potential of various deep learning architectures for this task. Salamon et al. developed a capsule neural network optimized with Bayesian optimization, achieving an accuracy of 95.1% on pediatric CXR images, with excellent sensitivity (98.9%) for detecting pneumonia cases [10]. Similarly, Khadidos et al. compared DenseNet121 and EfficientNet-B0 architectures, reporting that EfficientNet-B0 achieved 84.6% accuracy with the added benefit of explainability through Grad-CAM and LIME visualizations that highlighted clinically relevant lung regions [7]. Another study evaluated DenseNet-169 with transfer learning, achieving 91.6% accuracy in classifying X-ray images as normal or pneumonia [6].

In a study closely related to our work, Sánchez et al. also used the Guangzhou dataset to develop classifiers based on both neural networks and k-nearest neighbors (K-NN). Their neural network classifier achieved an accuracy of 96.9%, which is identical to our results, while their K-NN approach reached 89%. This reinforces the robustness of the neural network approach on this specific dataset and provides a direct point of comparison for our feature-based methodology [11].

Ensemble methods have also shown promising results. Harib et al. proposed a Dirichlet-evidence ensemble approach that incorporates uncertainty and selective prediction, achieving 100% accuracy on decided cases while abstaining on only 1-2% of uncertain studies, demonstrating a clinically safer deployment strategy [4]. A study using Maccabi Healthcare Services data in Israel validated a deep learning model on 537 pediatric CXRs, achieving 89.4% accuracy with 92.0% precision and 99.6% specificity when compared to radiologist consensus [5].

A critical observation in the literature is the predominant reliance on a single publicly available dataset. According to a recent scoping review by Rickard et al. that analyzed 35 studies published between 2018 and 2025, 31 of these studies used the Kermany dataset from the Guangzhou Women and Children's Medical Center—the same dataset used in the present study [9]. This raises concerns about overfitting and limited generalizability to broader, realworld clinical populations. The same review reported a median accuracy of 92.3% for binary classification (viral vs. bacterial pneumonia) and 91.8% for multiclass classification (normal, viral, bacterial) across the included studies [9]. A related review by Ye and Zhou further emphasizes that while AI tools have been validated to quickly analyze chest images and patient data, the development of high-quality, multicenter datasets remains essential for improving model interpretability and clinical adoption [13].

In contrast to the prevailing trend of end-to-end deep learning models that operate directly on raw images, the present study adopts a hybrid approach. First, seven texture features (mean, standard deviation, entropy, contrast, correlation, energy, and homogeneity) are extracted from CXR images using a MATLAB routine. These features are then fed into a simple feed-forward neural network for classification. This approach offers two key advantages: (1) it provides a more interpretable model by relying on radiologically meaning-ful features, and (2) it is computationally less expensive, making it suitable for deployment in resource-limited settings. While deep learning models like those in [7;10] achieve high accuracy, they often function as "black boxes," whereas our feature-based approach maintains a clearer link to the underlying radiological characteristics of pneumonia.

4. Materials and Methods

This section describes the methodological framework used to develop and evaluate the proposed pediatric pneumonia classifier. All image processing, feature extraction, and neural network implementation procedures were carried out in MATLAB. The methodology was structured into four main phases: dataset preparation, feature extraction, neural network design, and performance evaluation.

4.1. Dataset Description

The dataset used in this study consisted of anteroposterior chest X-ray images from retrospective cohorts of pediatric patients aged one to five years. The images were obtained from the publicly available pediatric pneumonia dataset from the Guangzhou Women and Children's Medical Center, which has been widely used in research on automated pneumonia detection.

The dataset composition is as follows:

- Normal cases: 49 images from children with no radiological evidence of pneumonia.
- Pneumonia cases: 48 images from children diagnosed with bacterial pneumonia.

This results in a total of 97 images. The dataset was randomly partitioned for each simulation run into training, validation, and testing subsets. No additional data augmen-tation techniques were applied to preserve the original image characteristics.

4.2. Feature Extraction

A custom MATLAB script was developed to read the chest X-ray images and extract seven texture features from each image. All images were processed in grayscale format. No additional preprocessing or data augmentation was applied in order to preserve the original characteristics of the images and maintain consistency across the feature extraction process.

The following MATLAB functions were used to extract the features:

- Mean: calculates the average pixel intensity, providing information about overall image brightness.
- Standard deviation: measures the dispersion of pixel intensities, indicating image contrast and variability.
- Entropy: quantifies the randomness or texture complexity of the image, which can differentiate between healthy and infected tissue patterns.

- Contrast, Correlation, Energy, and Homogeneity: these four features are derived from the Gray-Level Co-occurrence Matrix (GLCM) and provide detailed texture analysis:
  - Contrast: measures local intensity variations.
  - Correlation: indicates linear dependencies between pixel intensities.
  - Energy: represents texture uniformity.
  - Homogeneity: measures the closeness of the distribution of elements in the GLCM to the GLCM diagonal.

These seven features were chosen based on their ability to characterize lung tissue texture, which differs between healthy and pneumonic lungs due to the presence of infiltrates and consolidations in infected cases. The extracted features for all images were compiled and exported to an Excel spreadsheet for subsequent analysis.

Table 1 presents the minimum and maximum values obtained for each feature across the entire dataset, illustrating the range of variability in the input data.

Table 1. Extracted features from chest X-ray images: minimum and maximum values.

Mean	Standard deviation	Entropy	Contrast	Correlation	Energy	Homogeneity
58.722966	25.4391131	6.55155542	105815.022	-0.0025452	1.7772E-07	0.005195399
154.142016	76.0842049	7.84158158	1056016.32	0.0004597	2.4625E-06	0.013891749

4.3. Neural Network Classifier Design

A feed-forward artificial neural network (ANN) with a single hidden layer was implemented using MATLAB's Neural Network Toolbox. This architecture was chosen for its ability to model non-linear relationships between input features and output classes while maintaining computational simplicity.

4.3.1. Network Architecture

- Input layer: Seven neurons corresponding to the seven extracted features (mean, standard deviation, entropy, contrast, correlation, energy, and homogeneity).
- Hidden layer: A single hidden layer where the number of neurons was systematically varied (from 3 to 9) to evaluate its impact on performance.
- Output layer: One neuron with a binary output, where:
  - 0 represents a normal diagnosis.
  - 1 represents bacterial pneumonia.

4.3.2. Training Parameters

- Learning algorithm: Scaled Conjugate Gradient Backpropagation, selected for its efficiency with small to medium-sized datasets and its faster convergence compared with standard gradient descent.
- Transfer functions: nonlinear transfer functions were used in the hidden layer, tangent sigmoid (`tansig`), and in the output layer, log-sigmoid (`logsig`), to enable nonlinear decision boundaries.
- Performance metric: Mean Squared Error (MSE), calculated as the average squared difference between network outputs and target values. Lower MSE values indicate better model fit.
- Data partitioning: for each simulation, the dataset was randomly divided as follows:
  - Training set: 70% of the data.
  - Validation set: 15% of the data.
  - Testing set: 15% of the data.

4.3.3. Experimental Setup

To identify the optimal network configuration, five independent simulations were performed for each hidden layer size, ranging from 3 to 9 neurons. In each simulation, the network was initialized with random

weights and biases, trained until convergence, and evaluated using the validation and testing subsets. The average training time, number of epochs, and MSE were recorded for each configuration. The best-performing network was then further analyzed using confusion matrices to assess classification accuracy, sensitivity, and specificity.

4.4. Performance Evaluation

Model performance was assessed using multiple metrics:

- Mean Squared Error (MSE): To evaluate the goodness-of-fit during training.
- Confusion matrices: To visualize classification results, showing true positives, true negatives, false positives, and false negatives.
- Overall accuracy: Calculated as the proportion of correctly classified cases (both normal and pneumonia) over the total number of cases.
- Training time and epochs: To evaluate computational efficiency.

The results from all configurations were compared to select the optimal network architecture, balancing high accuracy, low computational cost, and minimal overfitting.

5. Results

This section presents the experimental results obtained from the neural network classifier. Performance was evaluated across different network configurations using Mean Squared Error (MSE), training time, number of epochs, and classification accuracy as key metrics. Unless otherwise stated, results are reported as averages over five independent simulation runs for each configuration.

5.1. Effect of Hidden Layer Size on Network Performance

To determine the optimal architecture, the number of neurons in the hidden layer was varied from 3 to 9. For each configuration, five simulations were conducted, and the average MSE, training time, and number of epochs were recorded.

Table 2 summarizes the performance metrics for each hidden layer size.

Table 2. Influence of the number of neurons in the hidden layer on network performance (average values over five simulations).

Number of neurons	MSE (average)	Training time (s)	Epochs
3	0.36304	3	26
4	0.00323	4	21
5	0.28748	5	8
6	0.005339	4	15
7	0.38392	4	8
8	0.20977	4	12
9	0.22833	2	3

As shown in Table 2, the configuration with 4 neurons in the hidden layer achieved the lowest average MSE (0.00323), indicating the best fit between network outputs and target values. The configuration with 6 neurons also performed well (MSE = 0.005339), while configurations with 3, 5, 7, 8, and 9 neurons exhibited considerably higher error rates. Training times were consistently low across all configurations, with the 9-neuron network training the fastest (2 seconds) but at the cost of higher MSE.

Figure 1 illustrates the optimal network architecture identified through this experimental process: a feed-forward neural network with seven input features, four neurons in a single hidden layer, and one binary output neuron.

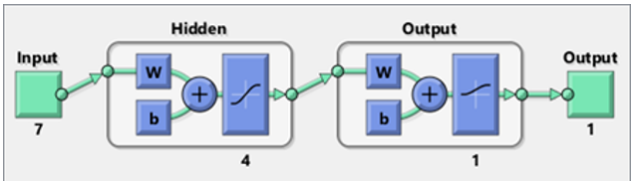

Figure 1. Optimal neural network architecture: seven input features, four hidden neurons, and one output neuron.

Figure 2. Confusion matrix for the network with three hidden neurons.

5.2. Classification Accuracy and Confusion Matrices

To further evaluate the performance of the best configurations, confusion matrices were generated for the networks with 3, 4, and 6 hidden neurons. These matrices provide a detailed view of correct and incorrect classifications for each class (normal and pneumonia).

Figure 2 presents the confusion matrix for the network with 3 hidden neurons.

The network with 3 hidden neurons achieved an overall accuracy of 89.7%. The highest performance was observed in the training subset, while validation and test accuracies were slightly lower.

Figure 3 presents the confusion matrix for the optimal network with 4 hidden neurons.

The network with 4 hidden neurons achieved an overall accuracy of 96.9%, with the highest performance observed in the validation subset. This configuration correctly classified the vast majority of both normal and pneumonia cases, with minimal false positives and false negatives.

Figure 4 presents the confusion matrix for the network with 6 hidden neurons.

The network with 6 hidden neurons achieved an overall accuracy of 93.9%. Notably, this configuration achieved 100% accuracy on both validation and test subsets, indicating excellent generalization, although the training accuracy was slightly lower.

5.3. Training Performance of the Optimal Network

Figure 5 shows the Mean Squared Error progression during training for one representative simulation of the optimal 4-neuron network. The plot demonstrates the convergence behavior, with the validation error stabilizing at a low value, indicating successful learning without significant overfitting.

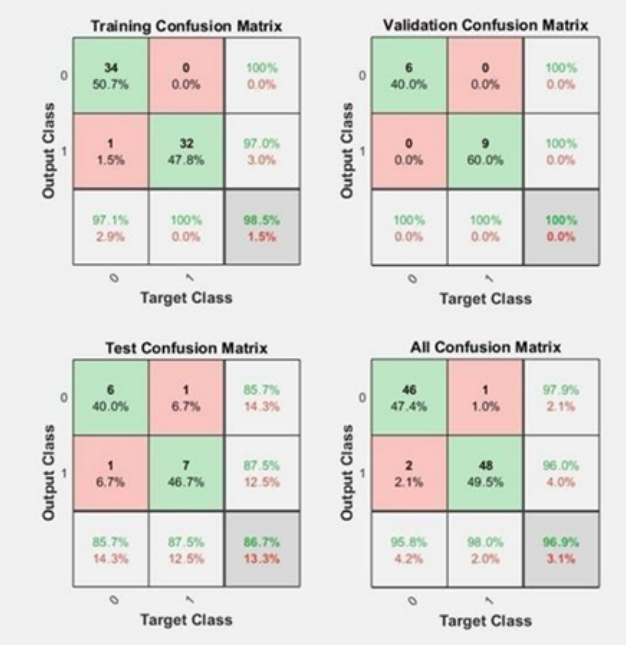

Figure 3. Confusion matrix for the network with four hidden neurons.

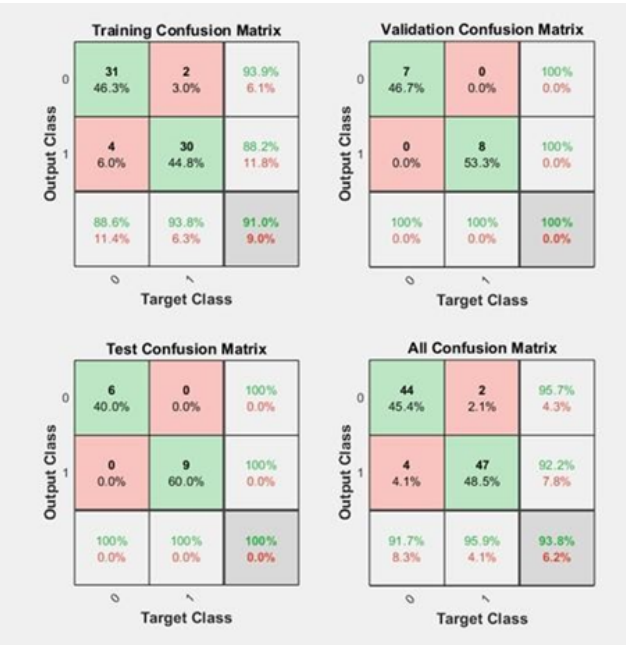

Figure 4. Confusion matrix for the network with six hidden neurons.

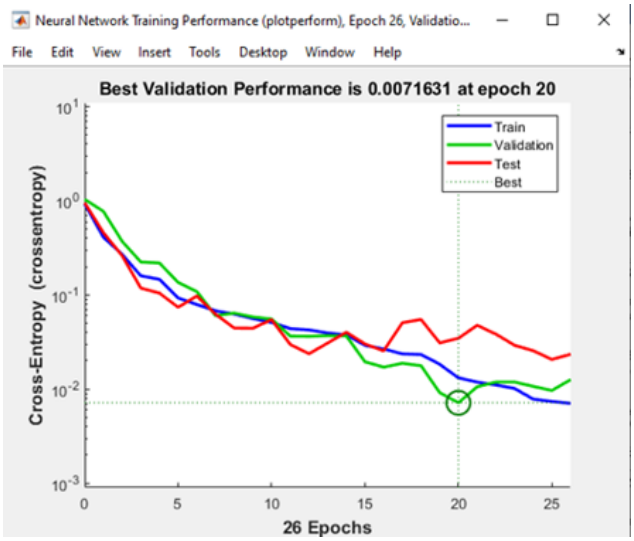

Figure 5. Mean Squared Error during training for the four-neuron network in a representative simulation.

6. Discussion

This study shows that a simple feed-forward neural network trained on seven manually extracted texture features from chest X-ray images can achieve high classification accuracy (96.9%) in distinguishing normal cases from bacterial pneumonia cases in a pediatric dataset. These results are relevant not only because of their diagnostic performance, but also because of their implications for model simplicity, computational efficiency, and interpretability in potential clinical decision-support settings.

6.1. Interpretation of Findings and Comparison with Previous Studies

The experimental results revealed that network performance is highly sensitive to the number of neurons in the hidden layer. The configuration with four neurons achieved the lowest MSE (0.00323) and the highest overall accuracy (96.9%), providing an optimal balance between underfitting and overfitting.

The 96.9% accuracy achieved in this study compares favorably with recent literature. (Salamon & Książek, 2025) reported 95.1% accuracy using capsule neural networks, while (Zhang et al., 2022) achieved 96.91% accuracy with fine-grained convolutional neural networks, results remarkably close to ours but achieved with significantly more complex architectures. Other studies have reported lower accuracies: (Khadidos et al., 2026) ob-tained 84.6% with EfficientNet-B0, and [6] achieved 91.6% with Dense-Net-169.

Notably, all these studies employed deep learning architectures operating directly on raw images, requiring substantial computational resources. In contrast, our approach achieves comparable accuracy using a simple neural network trained in seconds, demonstrating that thoughtful feature engineering remains valuable, particularly when computational resources or data are limited.

6.2. Advantages and Limitations

The proposed method offers three distinct advantages: first, interpretability as decisions can be traced to radiologically meaningful features. Second, computational efficiency with training times under five seconds and third, data efficiency achieving high accuracy with only 97 images.

However, several limitations should be acknowledged. First, the dataset comprised only 97 images from a single institution, which limits the statistical robustness of the results and restricts the generalizability of the model to broader clinical populations. Although the achieved accuracy was high, the small dataset size increases the risk that performance may be influenced by the specific characteristics of the selected images. Second, the model performs only binary classification, distinguishing normal cases from bacterial pneumonia cases, and therefore does not address viral pneumonia, mixed infections, or other thoracic pathologies that may appear in real clinical practice. Third, no systematic feature selection procedure was

performed, and additional radiomic, morphological, or texture-based descriptors could potentially improve model performance. Fourth, the model lacks external validation on independent, multi-institutional datasets, which is essential before considering clinical deployment. Therefore, the results should be interpreted as preliminary evidence of technical feasibility rather than as definitive proof of clinical applicability.

From a clinical perspective, the main challenge lies in translating the model's performance from a controlled experimental dataset to heterogeneous real-world healthcare environments. Chest X-ray images may vary according to acquisition protocols, equipment quality, patient positioning, disease severity, and the presence of comorbidities. These variations may affect the stability of handcrafted texture features and, consequently, the classifier's performance. For this reason, future validation should include larger and more diverse datasets, ideally from multiple institutions and different geographic contexts. Such validation would make it possible to assess the model's robustness, reduce the risk of dataset specific bias, and determine whether the classifier can support decision-making in resource-limited settings without replacing expert clinical judgment.

6.3. Future Research Directions

Based on these findings, several directions for future research are proposed. First, the model should be externally validated using larger, multi-institutional datasets. Second, the classification task should be expanded to include multiclass scenarios, such as normal, bacterial pneumonia, and viral pneumonia. Third, additional texture descriptors, particularly Local Binary Patterns (LBP), should be explored. Fourth, systematic comparisons with deep learning approaches should be conducted, evaluating not only accuracy but also interpretability, computational cost, training requirements, and clinical usability.

7. Conclusions

This study developed and evaluated a neural network-based classifier for childhood pneumonia diagnosis using chest X-ray images. By extracting seven texture features from a dataset of 97 images, a feed-forward neural network with a single hidden layer was implemented and assessed. The optimal configuration, consisting of four neurons in the hidden layer, achieved an overall classification accuracy of 96.9% and an MSE of 0.00323. These findings suggest that combining classical texture features with a simple neural network architecture can provide an efficient and interpretable approach for computer-aided diagnosis.

The proposed method offers practical advantages, particularly in terms of computational efficiency, interpretability, and data efficiency. These characteristics make it poten-tially useful in resource-limited healthcare settings where access to expert radiological interpretation may be constrained. Compared with more complex deep learning approaches reported in the literature, the results indicate that simpler feature-based models may still represent valuable tools in medical image analysis.

Nevertheless, the findings should be interpreted with caution. The dataset was relatively small and originated from a single institution, which limits the generalizability of the model to broader clinical populations. In addition, the current binary classification excludes viral pneumonia, mixed infections, and other thoracic conditions that may be encountered in routine clinical practice. Future work should focus on external validation using larger and more diverse datasets, expansion to multiclass classification, and the evaluation of additional texture descriptors such as Local Binary Patterns (LBP). Despite these limitations, the study provides preliminary evidence that an interpretable and computationally efficient neural network classifier can support the development of accessible diagnostic tools for underserved settings.

Author Contributions: **Fredy Munera Romero:** Conceptualization, Methodology, Software, Validation, Formal analysis, Investigation, Resources, Data curation, Writing – original draft, Writing – review & editing, Visualization, Project administration. **Adrian Gómez Consuegra:** Conceptualization, Methodology, Software, Validation, Formal analysis, Investigation, Resources, Data curation, Writing – original draft, Writing – review & editing, Visualization, Project administration.

All authors contributed equally to this work. All authors have read and agreed to the published version of the manuscript. Please refer to the CRediT taxonomy for the definitions of the terms. Authorship should be limited to those who have made substantial contributions to the reported work.

Funding: This research received no external funding.

Institutional Review Board Statement: Not applicable, since the present study does not involvehuman personnel or animals.

Informed Consent Statement: This study is limited to the use of technological resources, so nohuman personnel or animals are involved.

Conflicts of Interest: Under the authorship of this research, it is declared that there is no conflict of interest with the present research.

References

1. Blasi Sanchiz, A. (2021). Classificaci'o d'imatges pel diagn'ostic de pneum'onia.
2. Chaguendo Sanchez, C. A. and Avirama Buitrago, J. A. (2020). Plataforma m'ovil para el diagn'ostico autom'atico de la neumon'ia a partir de radiograf'ias tor'acicas soportada en deep learning.
3. Godoy Francisco, V. L. (2020). Algoritmo de diagn'ostico preliminar de neumon'ia a partir de im'agenes radiogr'aficas del t'orax.
4. Harib, W., Fouad, S., and Mahmoud, T. F. (2026). A dirichlet distribution-based trust-adaptive ensemble approach for pneumonia classification from chest x-ray images. In *IEEE International Symposium on Biomedical Imaging (ISBI)*. IEEE.
5. International Society for Pharmacoeconomics and Outcomes Research (2026). Evaluating a deep learning model for classifying pediatric pneumonia in israel. Retrieved March 6, 2026.
6. Katreddi, S., Midatani, A., Roy, A. P., Velpuri, U., and Kasani, S. (2025). Pediatric pneumonia x-ray image classification: Predictive model development with densenet-169 transfer learning. *Journal of Medical Artificial Intelligence*, 8(0).
7. Khadidos, A. O., Nanyonga, A., Khadidos, A. O., Mirza, O. M., and Yilmaz, M. T. (2026). Explainable deep learning for pediatric pneumonia detection in chest x-ray images.
8. Naar P'erez, A. and Barreto Mart'inez, F. (2019). Modelo de red neuronal convolucional para el diagn'ostico de neumon'ia en im'agenes radiol'ogicas.
9. Rickard, D., Kabir, M. A., and Homaira, N. (2025). Machine learning-based approaches for distinguishing viral and bacterial pneumonia in paediatrics: A scoping review. *Computer Methods and Programs in Biomedicine*, 268:108802.
10. Salamon, S. and Ksią.zek, W. (2025). Capsule neural networks with bayesian optimization for pediatric pneumonia detection from chest x-ray images. *Journal of Clinical Medicine*, 14(20):7212.
11. S'anchez, J. M. B., Villag'omez, J. L., Moreno, A. L., and Jim'enez, L. M. (2024). The development of a classifier based on neural networks and k-neighbors for pediatric pneumonia diagnosis through x-ray images.
12. Tapia Vargas, G. R. (2015). Utilidad de la radiograf'ia de t'orax en el diagn'ostico de neumon'ia en pacientes pedi'atricos, de 2 a 5 a nos; del hospital iii yanahuara, arequipa–per'u.
13. Ye, Y. and Zhou, W. (2026). Artificial intelligence in the diagnosis and prognosis of pediatric bacterial pneumonia: Current advances and challenges. *Current Opinion in Pediatrics*, 38(2):149.

Authors' Biography

Fredy Munera Romero Systems Engineering Student.

Adrian Gómez Consuegra Systems Engineering Student.